

Experimental determination of the tire-road friction coefficient for a vehicle with anti-lock braking system

Cite as: AIP Conference Proceedings 2557, 030001 (2022); <https://doi.org/10.1063/5.0103769>
Published Online: 13 October 2022

Hristo Uzunov, Kaloyan Dimitrov and Silvia Dechkova



View Online



Export Citation

1.8 GHz

8.5 GHz

Trailblazers. New

Meet the Lock-in Amplifiers that measure microwaves.

Zurich Instruments [Find out more](#)

Experimental Determination of the Tire-Road Friction Coefficient for a Vehicle with Anti-Lock Braking System

Hristo Uzunov^{a)}, Kaloyan Dimitrov^{b)}, Silvia Dechkova^{c)}

Technical University of Sofia, Faculty and College – Sliven, Bulgaria

^{a)} Corresponding author: hvuzunov@gmail.com

^{b)} ka_dimitrov@mail.bg

^{c)} si_yana@abv.bg

Abstract. In the present study, technical analysis of an experimental research has been carried out to verify tire-road friction coefficient of a vehicle with an anti-lock braking system (ABS) in the process of maximum braking force and in different types of surfaces. The study was conducted using three independent methods, including effective braking distance reading, deceleration measurement with an accelerometer, and a numerical experiment to study vehicle deceleration. The obtained polynomial determined the dependence of the coefficient of friction as a function of the velocity of the center of mass. Verification of experimental results from the first and second experiment was carried out by numerical analysis on the vehicle's deceleration implementing mechanical-mathematical model with ABS module. The results obtained from both the conducted experiment and numerical analysis on tire-road friction coefficient were processed by the methods and means for statistical analysis and expert assessments to determine the extent of results validity and credibility of the performed experiments. Considering the conducted dynamic study on the vehicle braking performance with an anti-lock braking system and the displayed graphic dependences, it has been proved that the maximum braking delay is achieved at constant pressure on the brake pedal. The coefficient of friction decreases with the increase of initial speed for different types of surfaces. High coefficient of friction is explained by the fact that the wheels of the car roll on the highest available slip and the coefficient of friction is similar to that at rest.

INTRODUCTION

This paper outlines a technical analysis of an experimental study performed on the friction coefficient of an automobile with an anti-lock system in the process of maximum braking force and on different types of road surface. The study is based on three independent methods, taking into account the length of the effective braking distance, using a special sensing device, an accelerometer PCE-MSR-145S-TA, and applying numerical experiment [1-3].

The purpose of the experiment is to investigate the dependence of the coefficient of friction in accordance with the speed of the car center of mass. The experimental data should also be verified by a numerical experiment of a developed dynamic model of a car equipped with an anti-lock system.

The absolute value (modulus) of the negative projection of the acceleration of the vehicle center of mass on the unit vector of the velocity direction is the known braking delay/negative acceleration/deceleration of the vehicle.

$$j = |a_{\tau}| = \left| \frac{dV}{dt} \right|. \quad (1)$$

Here, $|a_{\tau}|$ is the absolute value of the projection of the acceleration of vehicle's center of mass on the single vector $\vec{\tau}$; V – velocity of the car center of mass.

It is well-known that vehicles with fitted anti-lock braking system achieve maximum braking delay at constant pressure on the brake pedal. The braking process is related to the fact that the wheels of the car roll on the sliding friction limit.

EXPERIMENTAL STUDY OF AUTOMOBILE DECELERATION USING ACCELEROMETRY

The aim of the present study is to determine the negative acceleration of a car in different types of pavements applying two independent methods and numerical analysis of the achieved results. To achieve the goal of the experiment, Skoda Rapid with an anti-lock braking system was used. Engine power is $90 \text{ hp}/4200 \text{ min}^{-1}$ torque $230 \text{ Nm}/1500 - 2500 \text{ min}^{-1}$, at a curb weight of 1260 kg . In the investigation, model Fulda Multiconrol H88 185/60R15 tires were used for dry and wet road, whereas for snow and ice road they were Fulda Kristal T84 185/60R15.

The tests were performed on a straight, flat section of road in conditions of different friction between the tires and the road surface: dry, wet, sandy, snowy asphalt, ice, respectively. The measurement is achieved at different initial speeds of the center of mass in the range from 20 to 90 km/h and maximum efficiency of the brake system, similar to the emergency braking (Fig. 1).

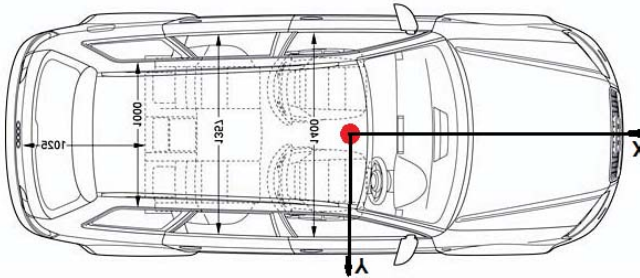


FIGURE 1. Location of the measuring device (accelerometer PCE-MSR-145S-TA).

Figures 2 to 6 show some graphical dependencies of the experimental data registered by the measuring device for the different types of pavements.

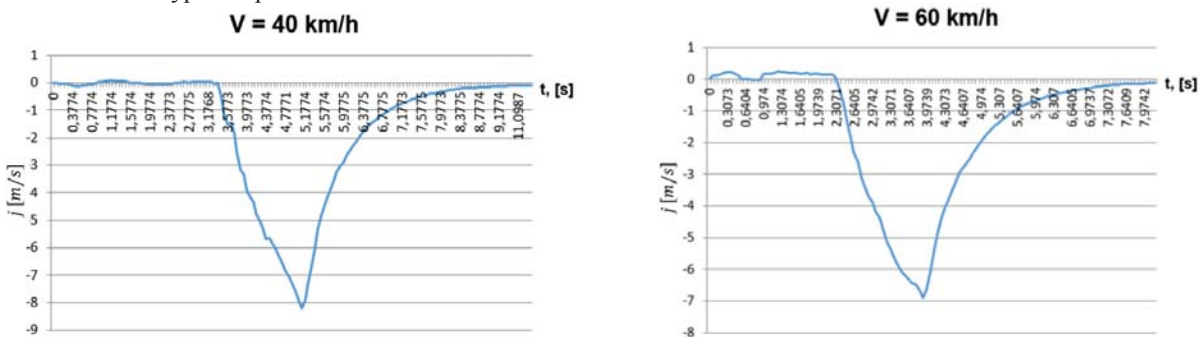


FIGURE 2. Graphical dependencies of the negative acceleration on dry road surface.

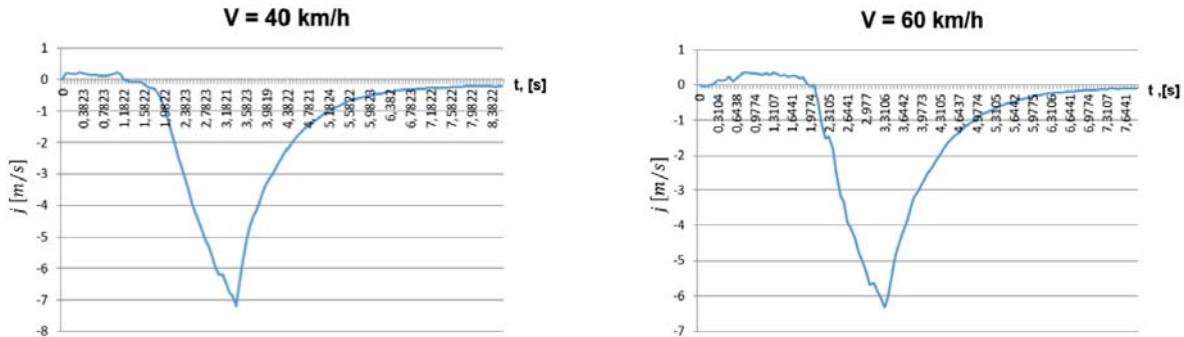


FIGURE 3. Graphical dependencies of the negative acceleration on wet road surface.

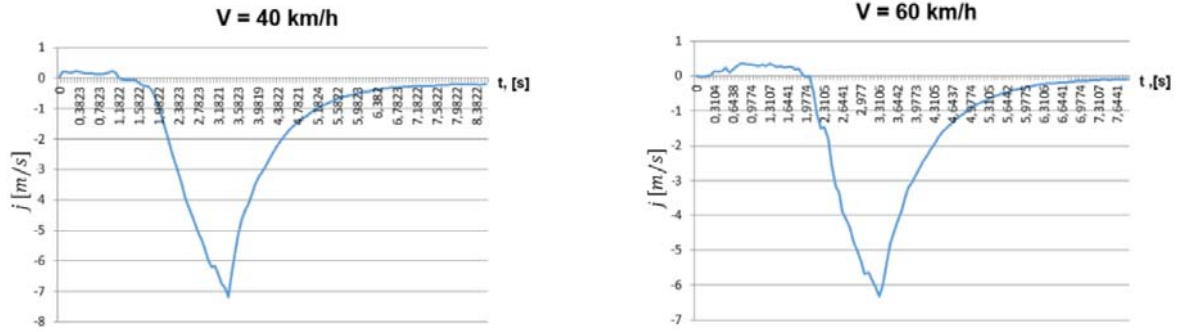


FIGURE 4. Graphical dependences of the negative acceleration on snowy road surface.

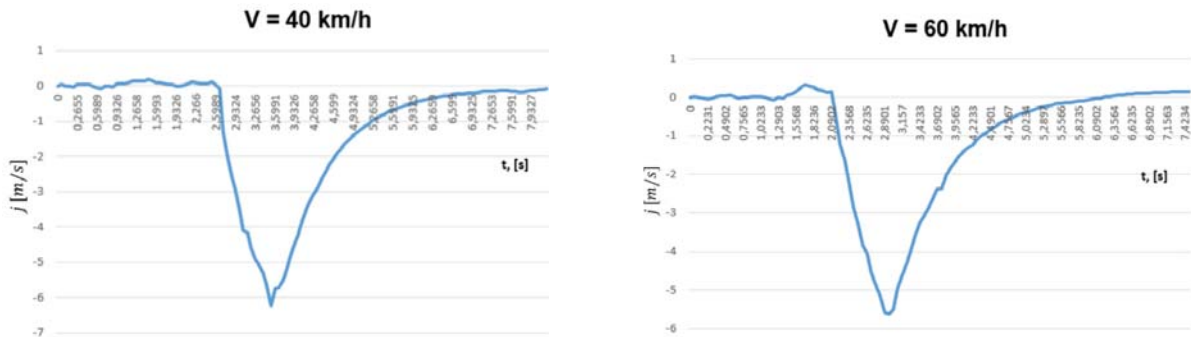


FIGURE 5. Graphical dependences of the negative acceleration on sandy road surface.

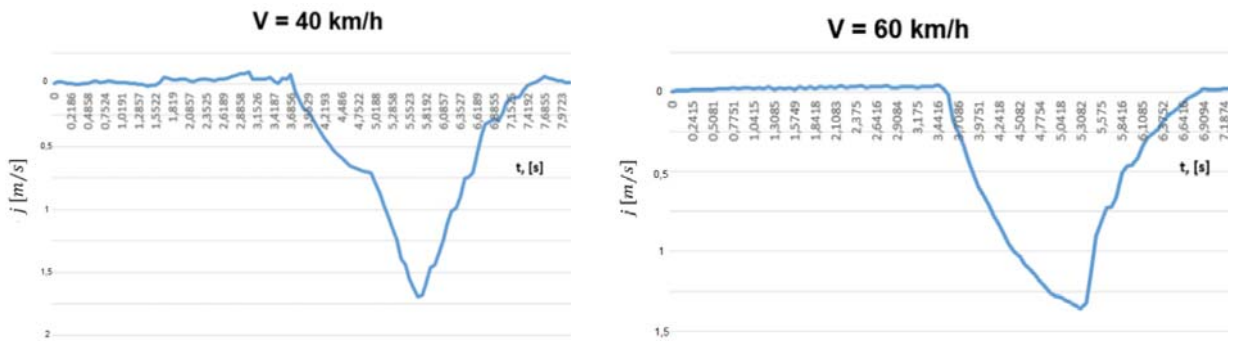


FIGURE 6. Graphical dependences of the negative acceleration on icy road surface.

Table 1 shows the obtained average values of the parameters in the set interval.

TABLE 1. Mean values of experimental data.

№	V, km/h	Road Surface				
		dry	wet	sandy	snowy	icy
		m/s^2	m/s^2	m/s^2	m/s^2	m/s^2
1	20	9,16	7,59	6,53	7,17	3,65
2	40	8,21	7,25	6,03	6,67	2,27
3	50	7,58	6,88	5,79	6,62	1,96
4	60	7,32	6,36	5,65	5,86	1,88
5	90	7,03	5,61	5,19	5,16	1,53

The average values obtained from Table 1 form a function of the form $y = f(x)$. Function approximation is sought in the form of Lagrange polynomial:

$$P_n(x) = a_0 + a_1x + a_2x^2 + \dots + a_nx^n \quad (2)$$

therefore,

$$P_n(x_i) = y_i, i = 0, 1, \dots, n.$$

The existence of such a polynomial is ensured by the following Lagrange interpolation polynomial, which has the form:

$$L_n(x) = \sum_{i=0}^n y_i \prod_{\substack{j=0 \\ j \neq i}}^n \frac{(x - x_j)}{(x_i - x_j)}. \quad (3)$$

The vehicle deceleration is displayed as a function of ground acceleration and the angle of inclination of the road and has the form of

$$j = (\mu \cos \alpha \pm \sin \alpha)g, \quad (4)$$

where μ – tire-road friction coefficient; α – angle of inclination of the road; g – ground acceleration.

From the performed experimental study a polynomial is obtained, which determines the dependence of the friction coefficient as a function of the velocity of the center of mass. It looks like:

dry road surface	$\mu_{11} = 7,80 \cdot 10^{-6} V^3 - 7,68 \cdot 10^{-4} V^2 - 2,62 \cdot 10^{-2} V + 9,93$	
wet road surface	$\mu_{12} = -1,57 \cdot 10^{-5} V^3 + 2,60 \cdot 10^{-3} V^2 - 9,60 \cdot 10^{-2} V + 6,58$	
sandy	$\mu_{13} = -1,03 \cdot 10^{-6} V^3 + 2,88 \cdot 10^{-4} V^2 - 4,02 \cdot 10^{-2} V + 7,23$	(5)
snowy	$\mu_{14} = -1,20 \cdot 10^{-5} V^3 + 2,03 \cdot 10^{-3} V^2 - 7,02 \cdot 10^{-2} V + 6,46$	
icy road surface	$\mu_{15} = 5,94 \cdot 10^{-4} V^2 - 9,44 \cdot 10^{-2} V + 5,24.$	

Graphical dependences on the tire-road friction coefficient are obtained (Fig. 7).

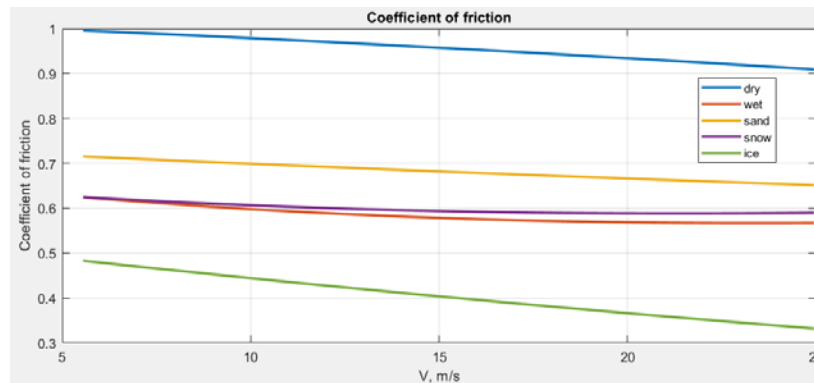


FIGURE 7. Graphical dependences of the coefficient of friction.

EXPERIMENTAL STUDY OF VEHICLE DECELERATION BY TAKING INTO ACCOUNT THE EFFECTIVE BRAKING DISTANCE

The experimental setup involves measuring the length of the effective braking distance according to a selected reference line, at different speeds of the center of mass in the selected range (Fig. 8).

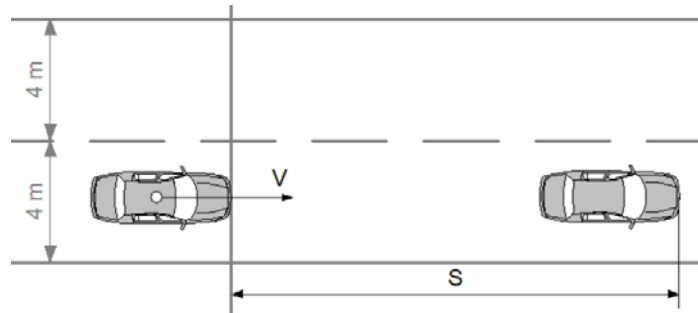


FIGURE 8. Scheme of conducting the experimental study.

The effective braking distance is determined by the length of the distance travelled at maximum pressure on the brake pedal. The dependence of the length of the effective braking distance of the car is determined by:

$$s = \frac{V_{bl}^2}{2j} = \frac{(V - 0,5t_H j)^2}{2j}, \quad (6)$$

where: V – initial speed of the experiment; V_{bl} – velocity of the vehicle's center of mass when the wheels are locked; t_H – time delay increase from zero to maximum; j – deceleration.

An equation determining deceleration is obtained

$$j = \frac{2s + t_H V - \sqrt{(2s + t_H V)^2 - t_H^2 V^2}}{0,5t_H^2}. \quad (7)$$

According to an experimental study, at each speed of the center of mass of the car, the average values of the length of the braking distance were taken into account. They are shown in tabular form.

TABLE 2. Average values of the braking distance.

№	$V, km/h$	Road Surface				
		dry	wet	sandy	snowy	icy
		S, m	S, m	S, m	S, m	S, m
1	20	0,80	1,25	1,70	1,75	4,00
2	40	5,40	7,20	9,40	9,30	18,20
3	50	9,10	12,30	16,20	17,50	30,10
4	60	14,20	19,10	24,10	26,30	49,90
5	90	35,20	48,30	56,30	62,30	122,00

From dependence (7) deceleration is calculated for the different type of road surfaces.

TABLE 3. Deceleration, m/s^2 .

№	$V, km/h$	Road Surface				
		dry	wet	sandy	snowy	icy
		m/s^2	m/s^2	m/s^2	m/s^2	m/s^2
1	20	8,92	7,74	6,27	6,45	3,51
2	40	8,28	7,02	5,61	5,80	3,24
3	50	8,24	6,74	5,29	5,03	3,10
4	60	8,00	6,45	5,23	4,90	2,72
5	90	7,80	6,01	5,21	4,78	2,52

The graphs of the coefficient of friction (Fig. 9) are in the form of a polynomial with respect to dependence (4). The polynomial takes the following form for the different types of road surface:

$$\begin{aligned}
 \text{dry road surface} & \quad \mu_{21} = -1,61 \cdot 10^{-4} V^3 + 1,01 \cdot 10^{-2} V^2 - 0,24 V + 9,95 \\
 \text{wet road surface} & \quad \mu_{22} = 6,55 \cdot 10^{-5} V^3 + 3,34 \cdot 10^{-5} V^2 - 0,14 V + 8,51 \\
 \text{sandy} & \quad \mu_{23} = -3,37 \cdot 10^{-5} V^3 + 6,58 \cdot 10^{-3} V^2 - 0,22 V + 7,35 \\
 \text{snowy} & \quad \mu_{24} = 6,51 \cdot 10^{-4} V^3 - 2,32 \cdot 10^{-2} V^2 + 0,10 V + 6,49 \\
 \text{icy road surface} & \quad \mu_{25} = 5,18 \cdot 10^{-4} V^3 - 2,24 \cdot 10^{-2} V^2 + 0,22 V + 2,86
 \end{aligned} \tag{8}$$

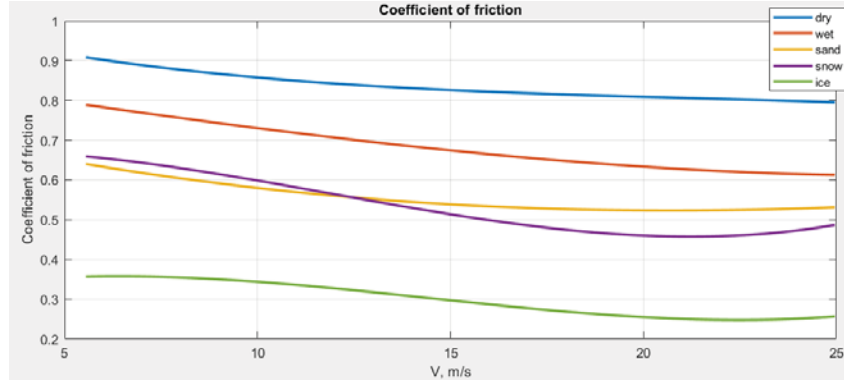


FIGURE 9. Graphical dependences of the coefficient of friction.

Having analysed the graphical dependences and after a comparative analysis with the experimental study using an accelerometer, a close arrangement of the graphs is seen for the different types of pavements in the selected interval of the speed of the center of mass [4, 5]. There are indicators showing the decreasing nature of the coefficient of friction in different types of pavements while increasing the speed of the center of mass, but with relatively high values.

NUMERICAL EXPERIMENT OF STUDYING VEHICLE DECELERATION BY DEVELOPING MATHEMATICAL MODEL OF MECHANICAL SYSTEMS WITH ABS MODULE

The relative motion of the wheels, differential/s and the engine is characterized by a system of four differential equations obtained by Lagrange method [6, 7], which has the type

$$[I_\gamma][\ddot{\gamma}] = [M_\gamma], \quad M_{\gamma i} = \{F_{i\tau}r_i + \text{sign}(\dot{\gamma}_i)[M_{di} - f_i N_i - M_{si}]\} \tag{9}$$

where: $\vec{F}_{i\tau}$ – tangential component of the friction force on the wheel; μ – coefficient of friction depending on the sliding speed of the contact spot, introduced graphically or analytically; r_i – radius of the wheel; f_i – coefficient of rolling friction; $[I_\gamma]$ – square matrix of coefficients in front of the actual angular accelerations of the drive wheels, depending on the wheel and engine inertia moments; $[\ddot{\gamma}]$ – matrix column of its own angular wheel accelerations, of which two or four are propulsive; M_{di}, M_{si} – corresponding engine and brake torque applied to each wheel.

$\vec{F}_{i\tau}$ is tangential component of the tire-road friction force, the positive direction of which is taken backwards, in the more frequent cases of braking or loss of stiffness.

$$F_{i\tau} = \mu N_i \left[\frac{V_{pix}}{V_{pi}} \cos(\varphi_z) + \frac{V_{piy}}{V_{pi}} \sin(\varphi_z) \right]. \tag{10}$$

Where $\mu(V_p)$ is friction coefficient depending on slipping speed on the contact spot; \bar{r}_i – radius of the wheel; f_i – coefficient of rolling friction; \bar{N}_i – normal reaction of the road on wheels.

The numerical experiment was performed on the basis of a developed ABS module. The change of the angular speed of the wheels and the braking torque is obtained as follows (Fig. 10):

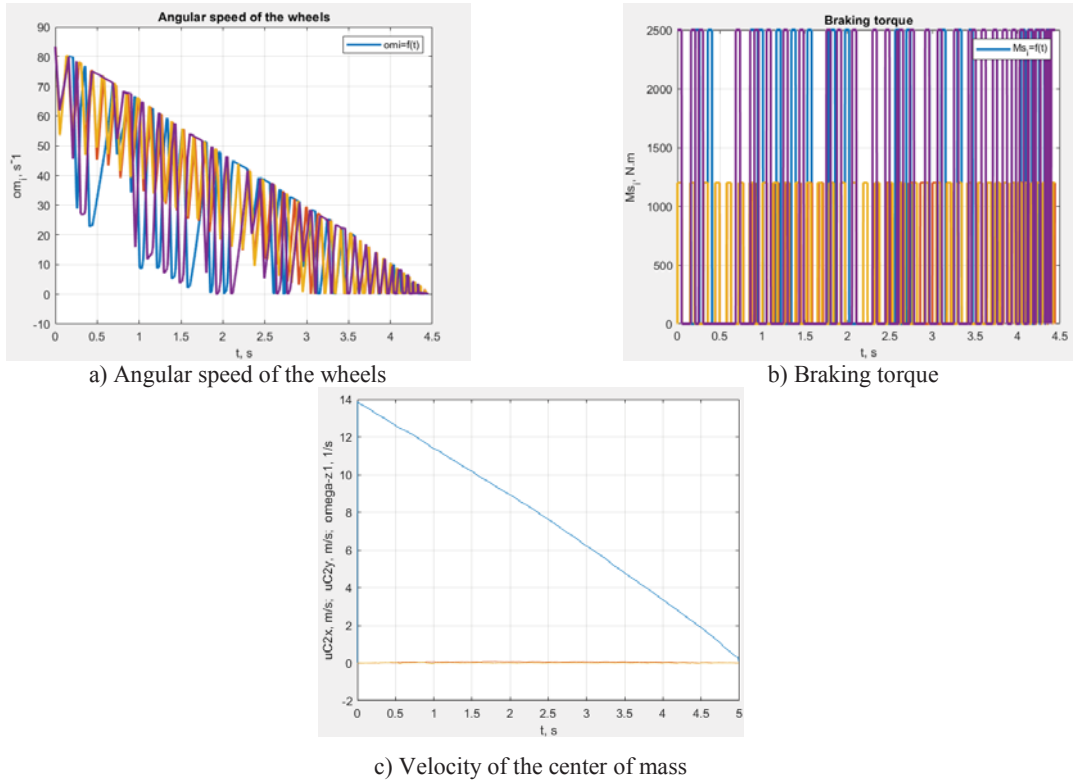


FIGURE 10. Graphical dependences on the change of the angular speed of the wheels and the braking torque.

Table 4 shows the values of the braking delay of the numerical test.

TABLE 4. Mean values of deceleration.

№	$V, km/h$	Road Surface				
		dry	wet	sandy	snowy	icy
		m/s^2	m/s^2	m/s^2	m/s^2	m/s^2
1	20	9,89	7,72	6,68	6,46	3,06
2	40	9,24	7,19	6,17	5,94	2,72
3	50	9,16	7,04	6,08	5,85	2,61
4	60	9,07	6,81	5,94	5,83	2,55
5	90	9,00	6,65	5,98	5,81	2,42

A polynomial is obtained determining the dependence of the coefficient of friction as a function of the velocity of the center of mass

$$\begin{aligned}
 \text{dry road surface} & \quad \mu_{31} = -3.05 \cdot 10^{-4} V^3 + 1,76 \cdot 10^{-2} V^2 - 0,34 V + 11,29 \\
 \text{wet road surface} & \quad \mu_{32} = 7,46 \cdot 10^{-5} V^3 - 5,29 \cdot 10^{-4} V^2 - 9,81 \cdot 10^{-2} V + 8,26
 \end{aligned} \tag{11}$$

sandy $\mu_{33} = -5,64 \cdot 10^{-5} V^3 + 5,66 \cdot 10^{-3} V^2 - 0,17 V + 7,46$

snowy $\mu_{34} = -2,78 \cdot 10^{-4} V^3 + 1,59 \cdot 10^{-2} V^2 - 0,29 V + 7,68$

icy road surface $\mu_{45} = -8,93 \cdot 10^{-5} V^3 + 5,81 \cdot 10^{-3} V^2 - 0,13 V + 3,67.$

Figure 11 shows the graphical dependences of the coefficient of friction depending on the speed of the car center of mass on different road surfaces.

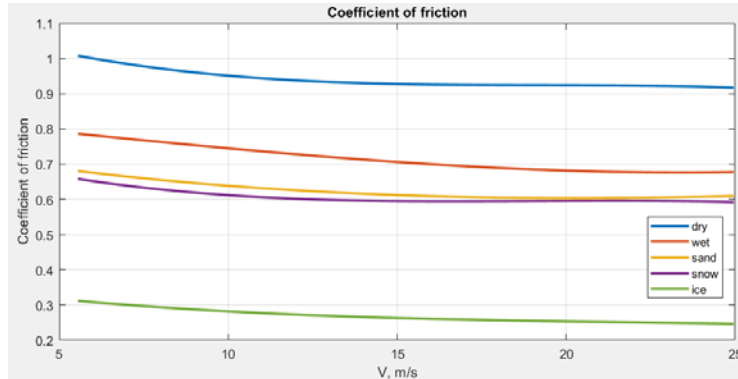


FIGURE 11. Graphical dependences of the coefficient of friction obtained in a numerical experiment.

ANALYSIS AND DISCUSSION OF THE OBTAINED RESULTS

The results obtained from the conducted experimental studies and numerical analysis of the tire-road friction coefficient and the road surface were processed [8-10]. Thus, the degree of reliability of the presented results can be determined.

Implementing the methods and means of mathematical statistics presented in [11, 12], the reliability of the presented results was proved, which provided the general set in the static analysis. The general population is a set of empirical data, derived from the solutions of the obtained polynomials and presented in Table 5.

TABLE 5. Empirical data for static analysis.

№	Coefficient of friction	Speed Of the Vehicle Center of Mass ($V, km/h$)				
		20	40	50	60	90
		<i>a</i>	<i>b</i>	<i>c</i>	<i>d</i>	<i>e</i>
1	μ_{11}	0,995	0,974	0,962	0,950	0,909
2	μ_{12}	0,624	0,592	0,582	0,574	0,567
3	μ_{13}	0,715	0,695	0,685	0,676	0,651
4	μ_{14}	0,625	0,603	0,595	0,591	0,589
5	μ_{15}	0,482	0,435	0,412	0,390	0,331
6	μ_{21}	1,007	0,943	0,930	0,925	0,917
7	μ_{22}	0,786	0,735	0,713	0,696	0,677
8	μ_{23}	0,680	0,631	0,616	0,607	0,609
9	μ_{24}	0,658	0,605	0,596	0,594	0,592
10	μ_{25}	0,312	0,276	0,266	0,259	0,246
11	μ_{31}	0,908	0,848	0,831	0,819	0,795
12	μ_{32}	0,788	0,716	0,685	0,658	0,612
13	μ_{33}	0,640	0,568	0,545	0,530	0,531
14	μ_{34}	0,659	0,579	0,531	0,489	0,487
15	μ_{35}	0,357	0,335	0,308	0,280	0,256

Table 6 shows the calculated value of the arithmetic mean for the representative sample of the measured values ($\bar{x}_a, \bar{x}_b, \bar{x}_c, \bar{x}_d$ and \bar{x}_e), which is the mathematical expectation μ of the means values by groups x_1, x_2, x_3, x_4 and x_5 . For the general population, the mathematical expectations x_1, x_2, x_3, x_4 and x_5 exist in the respective confidence intervals with 95% confidence probability [13, 14].

TABLE 6. Worksheet for calculating the standard deviation of the measured quantity.

№	a			b			c			d			e			Xabcde
	X_a	$(x_a - \bar{x})$	$(x_a - \bar{x})^2$	X_b	$(x_b - \bar{x})$	$(x_b - \bar{x})^2$	X_c	$(x_c - \bar{x})$	$(x_c - \bar{x})^2$	X_d	$(x_d - \bar{x})$	$(x_d - \bar{x})^2$	X_e	$(x_e - \bar{x})$	$(x_e - \bar{x})^2$	
1	0,995	0,312	0,097	0,974	0,338	0,114	0,962	0,344	0,119	0,950	0,347	0,120	0,909	0,324	0,105	0,958
2	0,624	-0,058	0,003	0,592	-0,043	0,001	0,582	-0,035	0,001	0,574	-0,028	0,000	0,567	-0,018	0,000	0,588
3	0,715	0,032	0,001	0,695	0,059	0,003	0,685	0,068	0,004	0,676	0,073	0,005	0,651	0,066	0,004	0,684
4	0,625	-0,057	0,003	0,603	-0,032	0,001	0,596	-0,021	0,000	0,591	-0,011	0,000	0,589	0,004	0,000	0,601
5	0,482	-0,199	0,040	0,435	-0,201	0,040	0,412	-0,205	0,042	0,391	-0,212	0,045	0,331	-0,253	0,064	0,410
1	1,007	0,324	0,105	0,943	0,307	0,094	0,930	0,312	0,097	0,925	0,322	0,104	0,917	0,332	0,110	0,944
2	0,786	0,103	0,010	0,735	0,099	0,009	0,713	0,096	0,009	0,696	0,093	0,008	0,677	0,092	0,008	0,721
3	0,680	-0,002	0,000	0,631	-0,004	0,000	0,616	-0,001	0,000	0,607	0,004	0,000	0,609	0,024	0,000	0,629
4	0,658	-0,024	0,000	0,605	-0,030	0,000	0,596	-0,021	0,000	0,594	-0,008	0,000	0,592	0,007	0,000	0,609
5	0,312	-0,370	0,137	0,277	-0,359	0,128	0,266	-0,350	0,123	0,259	-0,343	0,117	0,246	-0,338	0,114	0,272
1	0,908	0,225	0,050	0,848	0,212	0,045	0,831	0,213	0,045	0,819	0,216	0,046	0,795	0,209	0,044	0,840
2	0,788	0,106	0,011	0,716	0,080	0,006	0,685	0,067	0,004	0,658	0,055	0,003	0,612	0,027	0,000	0,692
3	0,640	-0,042	0,001	0,568	-0,067	0,004	0,545	-0,072	0,005	0,530	-0,072	0,005	0,531	-0,053	0,002	0,563
4	0,659	-0,023	0,000	0,579	-0,056	0,003	0,531	-0,086	0,007	0,489	-0,113	0,012	0,487	-0,097	0,009	0,549
5	0,357	-0,325	0,106	0,335	-0,301	0,090	0,308	-0,309	0,095	0,280	-0,322	0,104	0,256	-0,328	0,107	0,307
	0,682			0,636			0,617			0,603			0,585			0,6370
			0,570			0,545			0,556			0,574			0,572	

Standard square deviation for group values at n unit values for x_a, x_b, x_c, x_d and x_e :

$$S_{x_i} = \sqrt{\frac{[\Sigma(x_a - \bar{x})^2 + \Sigma(x_b - \bar{x})^2 + \Sigma(x_c - \bar{x})^2 + \Sigma(x_d - \bar{x})^2 + \Sigma(x_e - \bar{x})^2]}{n - 1}} = 0,19 \quad (12)$$

Standard deviation of the mean group values at n unit values for x_a, x_b, x_c, x_d and x_e :

$$s_{\bar{x}} = \frac{s_{x_i}}{\sqrt{n}} = \frac{0,1952}{\sqrt{5}} = 0,08 \quad (13)$$

Confidence interval:

$$q_{\bar{x}} = t \cdot s_{\bar{x}} = 2,57 \cdot 0,0873 = 0,22 \quad (14)$$

where: t is a coefficient which is a function of the statistical certainty S and of the number of unit values (experiments) n , therefore $t = 2,57$ at $S = 95\%$ and $n = 5$; $s_{\bar{x}}$ - of the average group values at n unit values for x_a, x_b, x_c, x_d and x_e :

Then the dependence for upper and lower limits is:

$$x_{ull} = \bar{x} \pm q_{\bar{x}}, \quad (15)$$

where \bar{x} is the arithmetic mean of the arithmetic means:

$$\bar{x} = \frac{\bar{x}_a + \bar{x}_b + \bar{x}_c + \bar{x}_d + \bar{x}_e}{n_i} = 0,62 \quad (16)$$

where n_i is the number of arithmetic means of the groups (x_a, x_b, x_c, x_d and x_e), or $n = 5$.

Then for the upper (17) and lower (18) limits we get:

$$x_{ul} = \bar{x} + q_{\bar{x}} = 0,6249 + 0,2243 = 0,84 \quad (17)$$

$$x_{ll} = \bar{x} - q_{\bar{x}} = 0,6249 - 0,2243 = 0,40 \quad (18)$$

Figure 12 shows the graph of the average values of the statistical indicators with upper and lower limits.

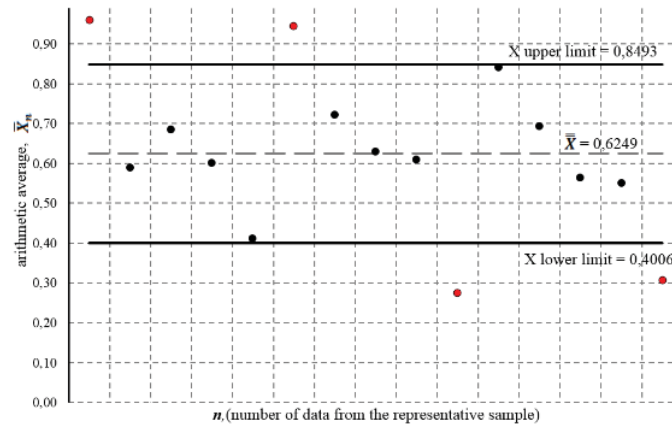


FIGURE 12. Graph for the average values of the measured quantities with upper and lower limits.

It can be seen that a large number of the average values fall within the confidence interval, which is a sufficiently satisfactory result. The values found between the limits of the confidence interval can serve as an arithmetic mean for the general population with a 95% confidence probability. This proves that the obtained experimental results for tire-road friction coefficient of the vehicle can be considered plausible.

CONCLUSIONS

An experimental and numerical study investigating braking acceleration of a car with an anti-lock braking system and on different types of pavements was conducted. Polynomial equations of friction coefficient dependences as a function of the automobile's center of mass velocity were derived. Graphical dependences were obtained by three different and independent methods, and the results were close in value.

The dynamic study of the friction coefficient pointed out that it decreased when increasing initial velocity of the center of mass. That was observed with all types of tested road surface. At low speed values, the coefficient of friction was significantly higher and close to that at rest. For the entire test interval, the relatively high coefficient of friction is explained by the fact that in the presence of an anti-lock braking system, the wheels of the car roll on the slip limit. Modern versions of anti-lock braking system implement the perfect option of the vehicle principle of operation, in which the system strives to maintain the friction coefficient close to that at rest.

A correlation analysis was performed, and the obtained results showed that a significant number of the average values fall into the confidence interval. It could be seen that between the limits of the confidence interval, the average values have a 95% confidence probability, which serves as an indicator of the reliability of the performed experimental study.

ACKNOWLEDGEMENTS

The author/s would like to thank the Research and Development Sector at the Technical University of Sofia for the financial support.

REFERENCES

1. R. Hegmon, T. Gillespie, and W. Meyer, "Measurement principles applied to skid testing", In *Skid Resistance of Highway Pavements*, edited by R. Wilcox, (West Conshohocken, PA: ASTM International), pp. 78–90 (1973).
2. R. Matsuzaki, K. Kamai and R. Seki, "Intelligent tires for identifying coefficient of friction of tire/road contact surfaces using three-axis accelerometer", *Smart Materials and Structures* **24**(2), 025010 (2014).
3. S. Hesapchieva, D. Hlebarski, G. Yanachkov, E. Dimitrov and Z. Georgiev, "Experimental study of motorcycle trim while braking" in *Proceedings of International Scientific Conference on Aeronautics, Automotive and Railway Engineering and Technologies BulTrans-2020*, pp. 106–113 (2020).
4. J. Cesbron, F. Anfosso-Lédée, D. Duhamel, H.P. Yin, D. Le Houédec, "Experimental study of tyre/road contact forces in rolling conditions for noise prediction", *Journal of Sound and Vibration* **320**(1–2), pp. 125–144 (2009).
5. R. van der Steen, I. Lopez and H. Nijmeijer, "Experimental and numerical study of friction and giffness characteristics of small rolling tires", *Tire Science and Technology* **39**(1), pp. 5–19 (2011).
6. S. Karapetkov, L. Dimitrov, Hr. Uzunov and S. Dechkova, "Identifying vehicle and collision impact by applying the principle of conservation of mechanical energy", *Transport and Telecommunication* **20**(3), pp. 191–204 (2019).
7. S. Karapetkov, L. Dimitrov, Hr. Uzunov, and S. Dechkova, "Examination of vehicle impact against stationary roadside objects", *IOP Conf. Ser.: Mater. Sci. Eng.* **659**, 012063 (2019).
8. M. D'Apuzzo, A. Evangelisti, V. Nicolosi, "An exploratory step for a general unified approach to labelling of road surface and tyre wet friction", *Accident Analysis & Prevention* **138**, 105462 (2020).
9. H. Mousavi, M.N. Shenvi and C. Sandu, "Experimental study for free rolling of tires on ice", in: *Proc. of the ASME 2019 Int. Design Eng. Technical Conf. and Computers and Information in Engineering Conf. Volume 3: 21st Int. Conf. on Advanced Vehicle Technologies; 16th Int. Conf. on Design Education*, Anaheim, California, USA. August 18–21, (2019).
10. Dh. Singh, H. Patel, A. Habal, A. Kumar Das, B.P. Kapgate, K. Rajkumar, "Evolution of coefficient of friction between tire and pavement under wet conditions using surface free energy technique", *Construction and Building Materials* **204**, pp. 105–112, (2019).
11. A. Abebe, J. Daniels, J.W. McKean, J. Kapenga, *Statistics and Data Analysis*, (Western Michigan University, Kalamazoo MI, 2001).
12. A. Delorme, *Statistical Methods*, (Swartz Center for Computational Neuroscience, INC, University of San Diego California, CA92093-0961, La Jolla, USA, 2016).
13. T.D. Gillespie, *Pavement Surface Characteristics and Their Correlation with Skid Resistance*, (Pennsylvania Transportation Institute, Transportation Research Building, University Park, PA United States 16802, 1964).
14. E. Ivanova, St. Tenev, T. Vasilev, "The theoretical model for determinig critical rotation speed flexible coupling type SEGE", *Scientific Bulletin of Naval Academy*, Vol. XXI, ISSUE no. 1, MBNA Publishing House Constanta, 4 c., ISSN 2392-8956, doi: 10.21279/1454-864X18-II-050, Romania, (2018).